

Biochemical and Spectroscopic Characterization of Highly Stable Photosystem II Supercomplexes from *Arabidopsis*

Aurelie Crepin, Stefano Santabarbara, Stefano Caffarri

▶ **To cite this version:**

Aurelie Crepin, Stefano Santabarbara, Stefano Caffarri. Biochemical and Spectroscopic Characterization of Highly Stable Photosystem II Supercomplexes from *Arabidopsis*. Journal of Biological Chemistry, 2016, 291 (36), pp.19157-19171. 10.1074/jbc.M116.738054 . cea-02160517

HAL Id: cea-02160517

https://cea.hal.science/cea-02160517

Submitted on 19 Jun 2019

HAL is a multi-disciplinary open access archive for the deposit and dissemination of scientific research documents, whether they are published or not. The documents may come from teaching and research institutions in France or abroad, or from public or private research centers.

L'archive ouverte pluridisciplinaire **HAL**, est destinée au dépôt et à la diffusion de documents scientifiques de niveau recherche, publiés ou non, émanant des établissements d'enseignement et de recherche français ou étrangers, des laboratoires publics ou privés.

THE JOURNAL OF BIOLOGICAL CHEMISTRY VOL. 291, NO. 36, pp. 19157–19171, September 2, 2016
© 2016 by The American Society for Biochemistry and Molecular Biology, Inc. Published in the U.S.A.

Biochemical and Spectroscopic Characterization of Highly Stable Photosystem II Supercomplexes from *Arabidopsis*[*S]

Received for publication, May 12, 2016, and in revised form, July 12, 2016 Published, JBC Papers in Press, July 18, 2016, DOI 10.1074/jbc.M116.738054

Aurelie Crepin[‡], Stefano Santabarbara[§], and Stefano Caffarri[‡1]

From the [‡]Aix Marseille Université, CEA, CNRS, BIAM, Laboratoire de Génétique et Biophysique des Plantes, Marseille 13009, France and the [§]Istituto di Biofisica, Consiglio Nazionale delle Ricerche, 20133 Milan, Italy

Photosystem II (PSII) is a large membrane supercomplex involved in the first step of oxygenic photosynthesis. It is organized as a dimer, with each monomer consisting of more than 20 subunits as well as several cofactors, including chlorophyll and carotenoid pigments, lipids, and ions. The isolation of stable and homogeneous PSII supercomplexes from plants has been a hindrance for their deep structural and functional characterization. In recent years, purification of complexes with different antenna sizes was achieved with mild detergent solubilization of photosynthetic membranes and fractionation on a sucrose gradient, but these preparations were only stable in the cold for a few hours. In this work, we present an improved protocol to obtain plant PSII supercomplexes that are stable for several hours/days at a wide range of temperatures and can be concentrated without degradation. Biochemical and spectroscopic properties of the purified PSII are presented, as well as a study of the complex solubility in the presence of salts. We also tested the impact of a large panel of detergents on PSII stability and found that very few are able to maintain the integrity of PSII. Such new PSII preparation opens the possibility of performing experiments that require room temperature conditions and/or high protein concentrations, and thus it will allow more detailed investigations into the structure and molecular mechanisms that underlie plant PSII function.

Photosystem II (PSII)[2] is the first complex involved in oxygenic photosynthesis. By using light energy, PSII is capable of extracting electrons from water and starting an electron transport chain that finally reduces carbon into organic matter through the Calvin-Benson cycle. This process sustains the vast majority of life on earth and produces the molecular O_2 necessary for aerobic metabolism.

PSII is a large membrane supercomplex composed of several protein subunits and cofactors (chlorophylls and carotenoid pigments, lipids, and ions). The supercomplex is organized in a dimeric form, with each monomer consisting of more than 20 subunits organized in two moieties: the core complex and the antenna system. The core complex is the only part well conserved among all oxygenic photosynthetic organisms (1). Conversely, the antenna systems are very different, being composed of integral membrane proteins in eukaryotes and peripheral proteins (phycobilisomes) in cyanobacteria (2). Significant differences in the organization of the antenna system can also be found in different eukaryotes as a result of different evolutionary pressures.

The core complex is composed of several subunits as follows: (i) D1 and D2, which contain the reaction center P680 and the cofactors of the electron transport chain; (ii) CP47 and CP43, which act as inner antennas by coordinating most of the core chlorophyll *a* molecules (Chls *a*), and (iii) several low molecular mass subunits, whose roles for the most part are only little understood (3, 4). Most of the differences between eukaryote and prokaryote core complexes are due to the presence in eukaryotes of additional low molecular mass proteins, such as PsbP, PsbQ, PsbR, PsbTn, and PsbW. Some of these proteins are involved in the stabilization of the oxygen-evolving complex (3, 5, 6) or the supercomplex (7).

A high resolution structure is of paramount importance for understanding the molecular mechanisms of PSII operation. However, only a high resolution atomic structural model of the cyanobacterial PSII core has been obtained so far. This was possible thanks to the isolation of PSII cores from thermophilic bacteria that are stable enough for the entire crystallization process. The crystallographic models so far have been obtained from cyanobacterial core complexes depleted of the phycobilisomes, because this type of antenna is easily detached from the reaction center. The structures show the positions of 35 Chl *a* molecules, 2 pheophytins, and 11–12 molecules of β-carotene (8, 9), as well as the position of other cofactors and the organization of the manganese cluster required for an efficient oxygen evolution and the position of the small subunits (10). However, no high resolution structural models are available for the eukaryotic PSII supercomplex, which has significant differences in protein and possibly also pigment content (11).

The first problem that needs to be solved to enable the structural determination of the eukaryotic PSII, as well as its functional characterization by biochemical and spectroscopic techniques, is the isolation of stable and homogeneous complexes. This task has proved to be not as straightforward as for PSII from thermophilic prokaryotes. The antenna system of eukaryotic PSII is composed of integral membrane proteins whose association to the core shows different degrees of strength (12,

* This work was supported by French National Research Agency Grant ANR-12-JSV8-0001-01 (to S. C.) and by A*MIDEX Project ANR-11-IDEX-0001-02 (to the Laboratoire de Génétique et Biophysique des Plantes). The authors declare that they have no conflicts of interest with the contents of this article.

[S] This article contains supplemental Table S1 and Figs. S1 and S2.

[1] To whom correspondence should be addressed. Tel.: 33-4-91-82-95-62; Fax: 33-4-91-82-95-66; E-mail: stefano.caffarri@univ-amu.fr.

[2] The abbreviations used are: PSII, photosystem II; CMC, critical micellar concentration; α-DDM, α-dodecyl maltoside; Tricine, *N*-[2-hydroxy-1,1-bis(hydroxymethyl)ethyl]glycine; Chl, chlorophyll; CHAPSO, 3-[(3-cholamidopropyl)dimethylammonio]-2-hydroxy-1-propanesulfonic acid; hexa-β-DM, *n*-hexadecyl-β-D-maltoside; Car, carotenoid; T, transmittance.

Downloaded from http://www.jbc.org/ by guest on June 19, 2019

13). In plants (as well in green algae), the antenna system is composed of the light-harvesting proteins ("Lhcb" for PSII), which have a primary role in light harvesting, transfer of excitation energy to the reaction center, and photosynthesis regulation via photoprotective mechanisms that dissipate the excess of energy absorbed as heat (non-photochemical quenching). The Lhcb proteins are coded by a multigenic family (14, 15) and coordinate Chl *a*, Chl *b,* and xanthophylls in different ratios. The major antenna complex, LHCII, is organized in heterotrimers composed of the products of the *Lhcb1–3* genes (16), whereas the three other subunits, CP29 (*Lhcb4*), CP26 (*Lhcb5*), and CP24 (*Lhcb6*; absent in green algae) are present as monomers (17). Monomers are directly associated to the core, whereas LHCII trimers can be either directly associated to the core or bound to the monomeric Lhcb complexes.

The supramolecular organization of PSII-LHCII (PSII core + antenna systems) has been investigated by electron microscopy (EM) and single particle analysis in plants (12, 18–20) and algae (21, 22). The larger supercomplex observed in *Arabidopsis thaliana* contains a dimeric core (C_2), two copies of the monomeric antenna complexes per dimer, two LHCII trimers (trimer S) strongly bound to the complex on the side of CP43 and CP26, and two more trimers, moderately bound (trimer M) in contact with CP29 and CP24. This complex is known as the $C_2S_2M_2$ supercomplex (13).

Attempts to obtain a high resolution structure of plant PSII by crystallization have been performed on core complex preparations, but with little success so far (23). It is likely that the protocol used to isolate PSII cores depleted of Lhc complexes, which requires quite harsh detergent treatments, causes PSII structural modification as well as heterogeneities that lead to low quality crystals or prevent crystallization. At the same time, the purification of homogeneous PSII-LHCII supercomplexes has proved to be extremely difficult due to the weak binding of part of the antennas that are lost during PSII purification.

An alternative approach to obtain structural models of PSII has been the use of electron microscopy; a 17-Å three-dimensional model by cryo-EM of PSII containing the two LHCII-S (the so-called C_2S_2 complex, which lacks CP24 and the LHCII-M trimers) has been obtained (24), as well as a 12-Å resolution model by a negative staining EM approach of the $C_2S_2M_2$ supercomplex, which also contains CP24 and the LHCII-M trimers (12). Very recently, the near atomic resolution of the spinach C_2S_2 supercomplex has been solved by using a cryo-EM approach (25). The protocol used for spinach PSII preparation by Wei *et al.* (25) is the one that we previously published for obtaining homogeneous preparations of *Arabidopsis* PSII supercomplexes with different antenna sizes (12). However, those preparations were stable only in cold conditions and for some tens of hours. Besides, it was not possible to concentrate the largest and complete $C_2S_2M_2$ supercomplex without causing significant degradation. These issues hampered the use of the full $C_2S_2M_2$ supercomplex preparation for in-depth structural and functional analysis. Because measurements on these samples could be performed only in cold conditions and on fresh non-concentrated samples, these were limited to negative staining EM (12) and time-resolved fluorescence spectroscopy (26). However, the smaller C_2S_2 supercomplex, containing the two strongly bound S-LHCII trimers, but lacking the moderately bound M-LHCII trimers and the monomeric CP24 antenna, was stable enough for its structural determination by single particle cryo-EM (25). In this work we present an improved protocol to obtain similar preparations as described previously (12), but with largely improved stability, thus allowing the use of these preparations for several different experiments that require room temperature conditions and/or at high protein concentration (up to ~6 mg/ml, or A_{cm} ~80).

We also investigated the biochemical and spectroscopic properties of the purified PSII supercomplexes. Finally, we tested PSII for stability in the presence of a large number of different detergents, and we found that very few are capable of maintaining the integrity of PSII. CHAPSO, *n*-hexadecyl-β-D-maltoside, and Pluronic F68 were determined to be the most efficient. Such a new preparation opens the possibility to investigate in much further detail the molecular mechanism underlying plant PSII activity by structural, functional, and spectroscopic techniques.

Results

Isolation of PSII Supercomplexes—Purification of plant PSII can be performed from thylakoid membranes or from PSII-enriched grana membranes (BBY, for the authors of the original protocol, Berthold, Babcock, and Yokum). The use of thylakoid can result in the contamination of PSII with other thylakoid complexes, especially PSI, which can dimerize and trimerize *in vitro* and comigrate with PSII supercomplexes (27). Although the successful preparation of pure PSII from thylakoid by sucrose gradient fractionation using α-DDM as detergent has been reported (28), we preferred to work with BBY membranes, whose preparation requires just a few hours more than thylakoid preparation and limits PSI contamination that would disturb biochemical and spectroscopic measurements.

To improve the stability of the PSII preparation with respect to the previous preparation (12), we changed the detergent used for solubilization and sucrose gradient fractionation. Rather than using α-DDM alone, which is a commonly employed detergent for the preparation of membrane proteins and supercomplexes, we used a mix of digitonin/α-DDM for membrane solubilization. Digitonin alone was then used at very low concentrations (0.01%) during sucrose gradient fractionation. Digitonin is a detergent that is commonly used for the preparation of membrane complexes and is bulkier and has milder solubilization properties than α-DDM. We previously used a similar protocol to prepare the PSI-LHCII supercomplex (27), a quite labile supercomplex that disassembles in the presence of α-DDM. Interestingly, during the membrane solubilization step, the presence of α-DDM in a mixture with digitonin has no detrimental effect on the supercomplex (27), rather its presence lead to two advantages as follows: (i) it allows a better solubilization of the membranes using less digitonin without affecting supercomplex integrity (27); (ii) it allows the use of a stock solution of digitonin, which is recommended to be freshly prepared to avoid detergent aggregation.

The exact solubilization conditions of the grana membranes (see "Experimental Procedures") are slightly different from the solubilization of thylakoid membranes for PSI-LHCII prepara-

Downloaded from http://www.jbc.org/ by guest on June 19, 2019

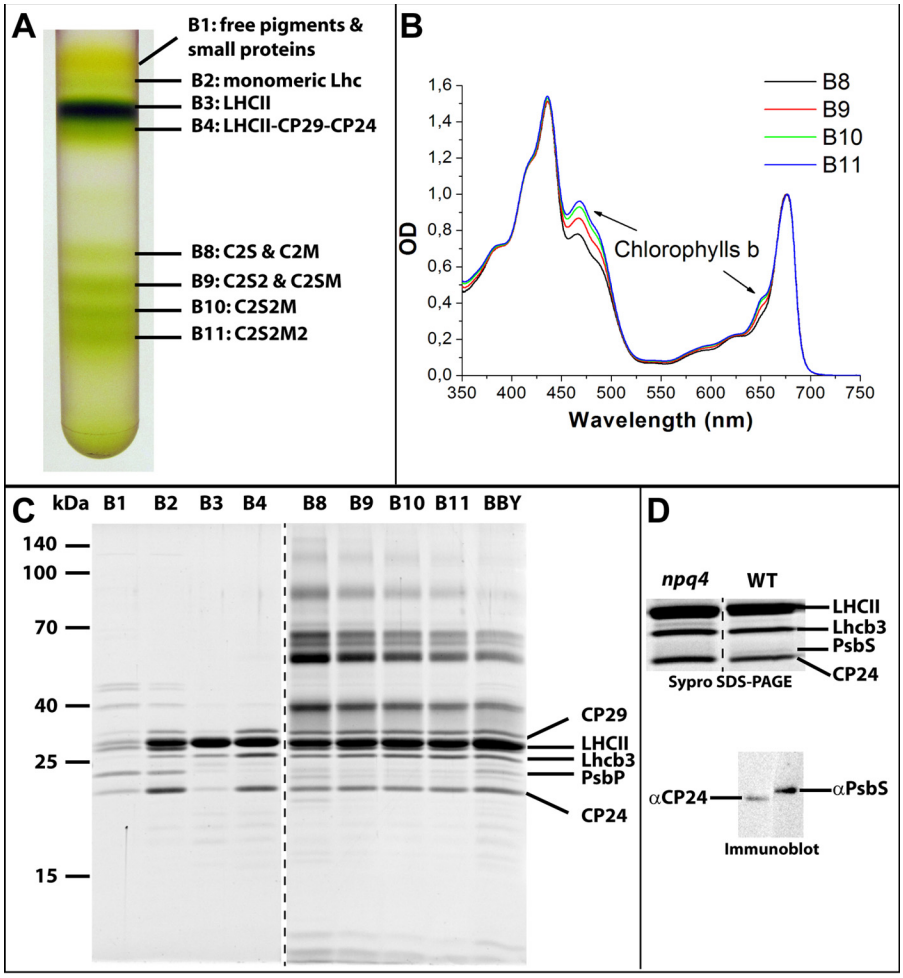


FIGURE 1. **Separation of PSII supercomplexes on sucrose gradient.** *A,* gradient separation of BBY membranes solubilized with 0.5% digitonin and 0.2% α-DDM. *Green bands* are labeled as in Ref. 12. PSII supercomplexes with increasing antenna size migrate in the B8 to B11 bands. *B,* absorption spectra of the B8–B11 fractions, normalized in the *red region*. The supercomplexes show an increasing absorption in the chlorophyll *b* regions, indicating an increasing number of LHCII trimers from B8 to B11. *C,* analysis by SDS-PAGE of the protein content of the purified fractions. The bands had globally the same composition as in Ref. 12. *D,* SDS-PAGE analysis of PSII from WT and *npq4* (koPsbS) plants. PsbS is visible as a very faint band above CP24 in the WT sample. The WT lane was then cut in half, and the identity of both CP24 and PsbS was confirmed by immunoblot.

tion (27) and have been optimized to maximize the yield of the largest PSII $C_2S_2M_2$ supercomplex. The sucrose gradient profile shown in Fig. 1*A* is almost identical to the one shown in Ref. 12, except for the lack of the B5 band (monomeric PSII core, C) and the extremely low concentration of B6 and B7 (the CS complex, a monomeric PSII core with one S-LHCII trimer attached, and the C_2 complex, the PSII dimeric core, respectively), due to the milder solubilization conditions.

As in Ref. 12, the absorption spectra of the bands indicate a Chl *b* content increasing with the molecular weight of the particles, which confirms an increasing antenna size (Fig. 1*B*). We maintained the same nomenclature as in Ref. 12, where we found that each fraction contains mainly C_2S (along with some C_2M) (B8), C_2S_2/C_2SM (B9), C_2S_2M (B10), and $C_2S_2M_2$ (B11) particles. The most abundant bands are B10 and B11, indicating that most, if not all, PSII in grana membranes of *Arabidopsis* plants grown under moderate light likely contain the M-LHCII trimer. Some M-trimer becomes unavoidably detached during the solubilization procedure, as demonstrated by the presence of the B4 band, a small supercomplex formed of M-LHCII, CP29, and CP24. The composition of B10 and B11 fractions was confirmed by electron microscopy single particle analysis (supplemental Fig. S1).

In addition to the absorption spectra, the composition of each band was investigated by SDS-PAGE (Fig. 1*C*). The results were again similar to the ones obtained in Ref. 12, with the notable exception of the B8 band, which showed a higher CP24 content than expected, suggesting higher retention of this protein with this purification protocol. This was confirmed by direct comparison on an SDS-polyacrylamide gel containing supercomplexes from both types of purification (supplemental Fig. S2).

The PsbS protein was present in the gradient fraction, as confirmed by SDS-PAGE and immunoblot analysis (Fig. 1*D*), although it only appeared as a very faint band, suggesting that it is present in substoichiometric amounts in the preparation. As for the α-DDM preparations of *Arabidopsis* analyzed by negative staining EM (12) and the same kind of preparation on spinach analyzed by cryo-EM (25), despite the presence of PsbS, we were not able to find a density corresponding to PsbS in negative-staining EM single particle analysis (supplemental Fig. S1). Further investigation is necessary to understand whether PsbS

Downloaded from http://www.jbc.org/ by guest on June 19, 2019

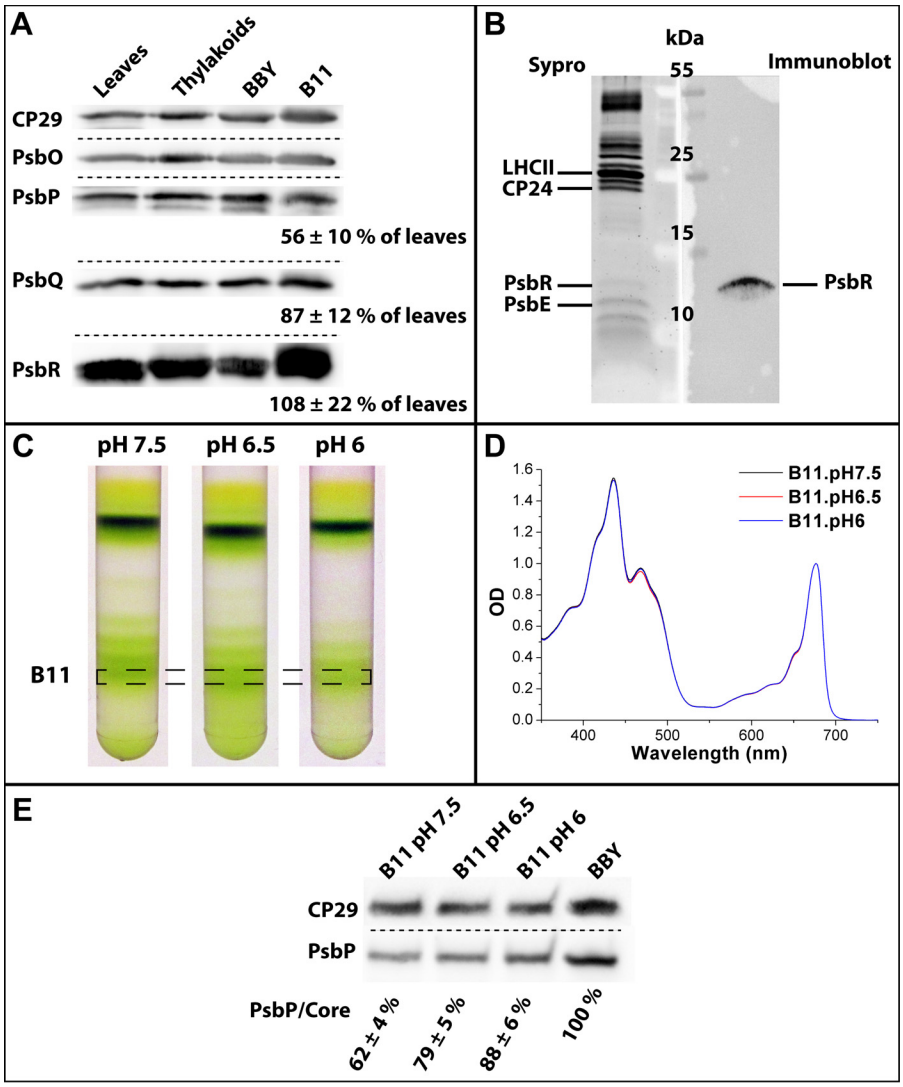


FIGURE 2. **Retention of peripheral subunits of PSII.** *A,* presence and quantity of the PsbP, PsbQ, and PsbR subunits in the purified supercomplexes were assessed by immunoblotting and compared with their quantity in membranes (BBY and thylakoids) and leaves (total proteins). The quantity of PsbP, PsbQ, and PsbR in the B11 fraction compared with leaves is indicated. CP29 and PsbO, which are present in one copy per monomeric PSII core, were used for normalization. *Error,* standard error of the mean, $n = 4$ (PsbP and PsbR) or $n = 3$ (PsbQ). *B,* PsbR was separated from PsbE on a Sypro-stained gel to estimate its stoichiometry. PsbR appeared as a fainter band than PsbE, an intrinsic PSII core subunit, suggesting a substoichiometric amount of PsbR. PsbR identity was confirmed by immunoblot analysis. *C,* BBY membranes were deposited on sucrose gradients containing, respectively, 10 mM Hepes, pH 7.5, 10 mM MES, pH 6.5 or 6. All three gradients showed a similar profile, although less material was solubilized at lower pH. *D,* absorption spectra of the B11 fractions purified from the different pH gradients, normalized on the *red peak*. The spectra of the three fractions are almost identical, indicating that low pH gradients contain intact $C_2S_2M_2$. *E,* PsbP quantity was assessed in PSII supercomplexes purified at different pH values. The quantity of PsbP as compared with grana membranes using CP29 for normalization is indicated. *Error,* standard error of the mean ($n = 8$).

just comigrates with PSII, is bound at several positions, or is in too low an amount and thus not easily visible in EM or bound to one position but detached during grid preparation.

Retention of Peripheral Subunits and O_2 Evolution—Most of the PSII subunits are integral membrane proteins whose presence in the supercomplex is detected by SDS-PAGE analysis and proteomic analysis (12, 20). However, the PsbP subunit, which belongs to the lumen-exposed oxygen-evolving complex, is a peripheral protein that was strongly depleted in our previous PSII preparation in α-DDM (12), but less depleted in a similar α-DDM preparation from Pagliano *et al.* (20). Small peripheral subunits, such as PsbQ and PsbR, are also easily lost during purification and are indeed absent from the supercomplexes described in other studies (20). To test whether our new digitonin preparation was more efficient in retaining these proteins, we performed an immunoblot analysis for all three proteins, along with the more stably attached PsbO and CP29 as control. Results show that PsbQ and PsbR are both retained in $C_2S_2M_2$ complexes as compared with thylakoids (Fig. 2*A*). Unfortunately, a significant part of PsbP was lost during purification, starting from thylakoid isolation. On average, about half of the initial PsbP content present in the leaves was retained in the purified $C_2S_2M_2$, which is a higher amount than in our previous PSII preparation (12).

As PsbR is retained in the purified PSII, we performed a semi-quantitative estimation of its stoichiometry in the particles. To this aim, PsbR was separated from PsbE, an integral core subunit that has a similar molecular mass (~10.2 and ~9.4 kDa, respectively) and that is present in one subunit per monomeric PSII. SDS-PAGE required a Tris-Tricine system, which allows

Downloaded from http://www.jbc.org/ by guest on June 19, 2019

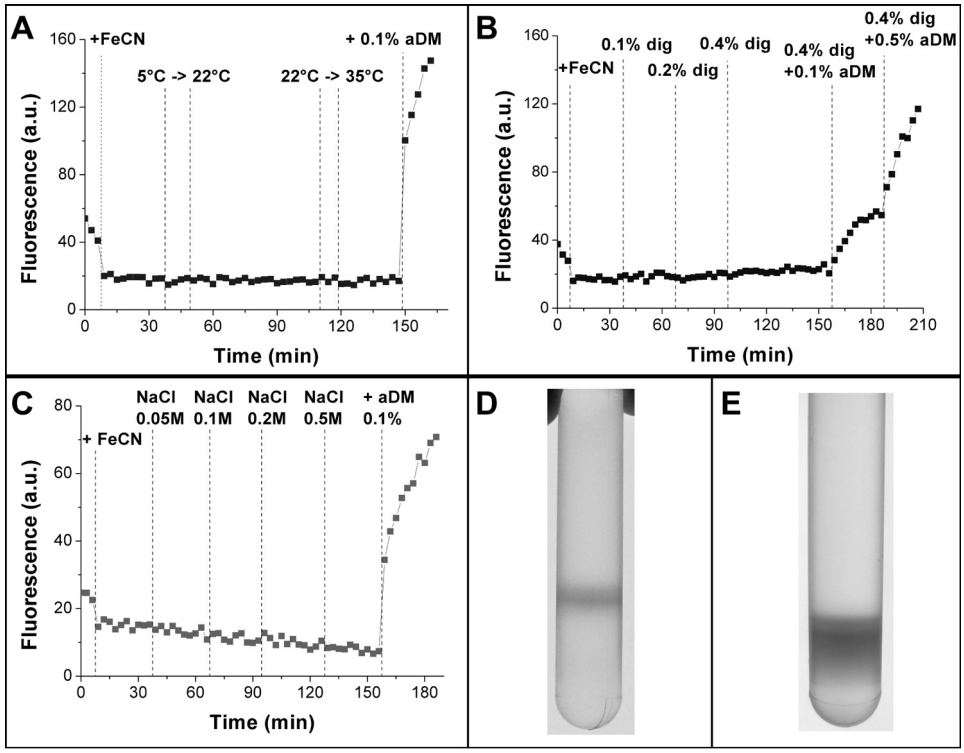


FIGURE 3. **Stability of the supercomplexes in different conditions.** Fluorescence emission changes of the $C_2S_2M_2$ supercomplex were measured by increasing temperatures (*A*), digitonin concentration (*B*), and NaCl concentration (*C*). Addition of α-DDM served as a control for the integrity of the complex, because it induces disassembly and increase of the fluorescence signal. *a.u.*, arbitrary units. *D*, purified B11 band was frozen, thawed, and concentrated/diluted to eliminate the sucrose and then deposited on a second gradient. No degradation of the complex was observed. *E*, B11 band was concentrated up to 6 mg/ml and deposited on a second gradient. No degradation of the complex was detected.

separating low molecular weight proteins, and PsbR identity was confirmed by immunoblot (Fig. 2*B*). As visible in Fig. 2*B*, PsbR is detectable on the gel, but it appears as a fainter band than PsbE. Considering that PsbR contains even more residues (Arg, Lys, and His) binding the Sypro staining than PsbE (11 and 7, respectively), it can be concluded that PsbR is present in a substoichiometric amount (<0.5 protein per monomeric core) in the PSII particles.

We investigated the effect of the pH on the retention of the PsbP protein in the purified PSII particles. We tested three different pH values as follows: 7.5 (the pH at which we usually purify the complex), 6.5, and 6. For an appropriate membrane solubilization, we had to increase the detergent concentration with the lowering of the pH, as shown previously (12). The profiles of the gradients were substantially equivalent in the three different conditions (Fig. 2*C*), as well as the absorption spectra of the bands (Fig. 2*D*), indicating that the Lhc content was not altered. We checked PsbP content in PSII particles prepared at these three pH values and compared it with the content in grana membranes. Fig. 2*E* shows that PsbP loss in PSII particles (by normalization on the PsbO subunit) is decreased by lowering the pH for the preparation, suggesting that the pH could have a role in PsbP binding to PSII and, as a consequence, in the stabilization of the oxygen-evolving complex.

We also measured O_2 evolution by $C_2S_2M_2$ particles. We found that PSII particles evolved 172 ± 19 μmol of $O_2 \cdot mg(Chls)^{-1} \cdot h^{-1}$, both in the case of the fraction collected from the gradient and after its concentration to 3.5 mg (Chls)/ml. This value was lower than the one measured on BBY membranes, which evolved O_2 at 270 ± 35 μmol of $O_2 \cdot mg(Chls)^{-1} \cdot h^{-1}$.

PSII Stability—We tested the stability of PSII supercomplexes using the largest $C_2S_2M_2$ particles, which are the most fragile ones due to the presence of two moderately bound M-LHCII trimers (12). The strategy was similar to that previously employed (12), which consisted of recording the kinetics of the steady-state fluorescence signal at 680 nm (maximum emission of LHCII) of the supercomplex during different treatments involving detergents, temperature, and salts (ionic force). Using a low intensity excitation light and in the presence of the artificial electron acceptor ferricyanide, PSII is substantially in an open state, and photochemistry quenches most of the energy harvested by the Lhc (because it is efficiently transferred to the core). However, detachment of antennas from PSII results in an increase in fluorescence yield due to the much longer excited state lifetime of Lhc complexes in solution as compared with PSII core complexes, thus allowing a simple measurement of PSII disassembly. We tested the stability of PSII at different temperatures, in the presence of increasing concentrations of digitonin, and increasing concentrations of NaCl. The detergent α-DDM was added at the end of each experiment to induce PSII disassembly and further control the integrity of PSII before this step.

As visible in Fig. 3*A*, PSII did not show any significant increase of the fluorescence signal even when held at 35 °C for several hours, a temperature much higher than room temperature, indicating a very good thermal stability for experiments

Downloaded from http://www.jbc.org/ by guest on June 19, 2019

that require room temperature. We also investigated the effect of increasing digitonin concentrations up to 0.4% at room temperature (Fig. 3*B*), and the results showed that even quite elevated digitonin concentrations have no appreciable effect on PSII integrity. Finally, we tested the effect of high salt (NaCl) concentrations up to 0.5 M. No detachment of Lhc was induced (Fig. 3*C*). However, the fluorescence signal decreased during the experiment, suggesting some aggregation of PSII. This phenomenon was further investigated, and the results are presented below. Freezing-melting of the sucrose gradient fractions also did not cause any disassembly of the PSII particles (Fig. 3*D*).

PSII Particle Concentration—PSII concentration in the sucrose gradient fractions is relatively low, and in the best cases and without overloading the gradient, which would reduce the purity of each fraction, it is possible to harvest bands at an $A_{680\,nm} \sim 1\ cm^{-1}$. For the $C_2S_2M_2$ particles, this corresponds to a concentration of about 75 μg/ml of the holocomplex, which is a concentration high enough for certain kinds of experiments, such as fluorescence spectroscopy, but too low for many other kinds of experiments, such as transient absorption spectroscopy. A previous preparation of PSII in α-DDM (12) was not suitable for concentration, because PSII disassembly was unavoidable during the procedure. In contrast, the new preparation in digitonin is much more stable and can be easily concentrated using centrifugal filter concentrators. At our working concentration (0.01%), digitonin should not form micelles (0.03% CMC); therefore, in principle the detergent should not concentrate even using filters with a low molecular weight cutoff. However, by trying concentrators of various brands and with different cutoffs (10, 30, and 100 kDa), we obtained different results, in particular for the aggregation of the sample. We found that the only filters that allow concentration to very high protein levels without any significant aggregation of PSII particles were Amicon 10-kDa filters (Millipore). It is not clear whether it is the material of the filter or the concentration of the digitonin itself that maintains the particles in solution (without detrimental effects on their integrity) or a combination of both effects.

In cases where it is necessary to remove the sucrose from the buffer, 3 or 4 dilution-concentration steps using a buffer containing 0.01% digitonin but no sucrose allowed the almost complete removal of sugar from the solution. In a similar way, it is also possible to change the buffer. Using this procedure, we were able to concentrate PSII particles up to $A_{680\,nm} \sim 80\ cm^{-1}$ (about 6 mg/ml holocomplex) without any disassembly of the supercomplex (Fig. 3*E*).

Pigment Content—The four PSII bands of the sucrose gradient and the grana membranes were analyzed by HPLC and spectrophotometric techniques to determine their pigment content (Table 1).

As expected, the Chl *a*/*b* ratio decreased inversely with the molecular weight of the particles, because Chls *b* are bound to the peripheral Lhc antenna system, whose number increases in the supercomplexes from B8 to B11. By normalizing the pigment content of each band to the number of Chls in each particle according to the calculated putative stoichiometry (42 Chls per LHCII trimer, 13 Chls per CP29 and CP26, 11 Chls per CP24, and 35 Chls per monomeric PSII core (11)), we can estimate the total pigment content of each PSII supercomplex (Table 1). The measured Chls and Cars content for B9, B10, and B11 bands corresponded well to that expected by calculations (see Table 1 in Ref. 11 for the case of $C_2S_2M_2$). In the case of BBY, the Chl *a*/*b* ratio and the pigment content normalized to four pheophytins (*i.e.* to a dimeric PSII) indicate that almost four more loosely bound LHCII trimers per dimeric PSII are present in membranes, confirming the results of previous publications (29–31).

TABLE 1
Pigment composition

The pigment content of the four fractions containing PSII supercomplexes (B8–B11), the LHCII trimers, and the BBY was analyzed by HPLC and spectroscopy and normalized to the number of chlorophylls per complex (A) or per 100 total Chls (B). Neo is neoxanthin; Vio is violaxanthin; Lut is lutein; β-car is β-carotene; Pheo is pheophytin. Total Cars indicates total carotenoids. Values are the averages of 3–6 measurements (error <5%).

A)	Neo	Vio	Lut	β-car	Chl a	Chl b	Pheo a	Chls a/b ratio	total Cars	n° Chls for normalization
B8	5.0	2.6	15.5	16.6	104.8	33.2	2.9	3.16	39.7	138
B9	7.6	4.0	23.9	18.3	145.2	54.8	3.9	2.65	53.7	200
B10	10.6	5.2	34.3	20.3	181.7	77.3	4.1	2.35	70.5	259
B11	13.9	6.6	43.0	21.8	213.4	98.6	4.0	2.16	85.2	312
BBY	27.5	11.0	79.9	23.1	318.6	161.4	4.0	1.97	141.4	480
LHCII	1.0	0.2	2.5	0.0	8.1	5.9	0.0	1.37	3.8	14
B)	**Neo**	**Vio**	**Lut**	**β-car**	**Chl a**	**Chl b**	**Pheo a**	**Chls a/b ratio**	**total Cars**	**n° Chls for normalization**
B8	3.6	1.9	11.2	12.0	76.0	24.0	2.1	3.16	28.8	100
B9	3.8	2.0	11.9	9.1	72.6	27.4	1.9	2.65	26.8	100
B10	4.1	2.0	13.2	7.8	70.2	29.8	1.6	2.35	27.2	100
B11	4.4	2.1	13.8	7.0	68.4	31.6	1.3	2.16	27.3	100
BBY	5.7	2.3	16.6	4.8	66.4	33.6	0.8	1.97	29.5	100
LHCII	7.5	1.5	18.1	0.0	57.8	42.2	0.1	1.37	27.1	100

By focusing on the largest $C_2S_2M_2$ particle, which we normalized to 312 total Chls, we found that almost 100 chlorophylls are Chls *b* and the remaining are Chls *a*. This supercomplex binds around 85 Cars in total, about half of which are lutein molecules that are bound to the antenna system together with ~14 neoxanthins and ~7 violaxanthins. The remaining carotenoids (~22 β-carotenes) are bound to the core complex. It can be calculated that for a $C_2S_2M_2$ particle, the pigments account for ~330 kDa of the ~1500-kDa holocomplex.

The measured B8 pigment content does not correspond to the expected value, in particular for the Chl *a*/*b* ratio (which is too low) and the low pheophytin content when normalized to the estimated Chls content per particle. Coupled with the SDS-PAGE results (see above and Fig. 1*C*), this suggests that this band contains mixed supercomplexes, possibly with a different ratio between C_2S and C_2M than previously observed (12) or a high content in CP24. We did not further analyze supercomplexes in the B8 band, because they are composed of mixed PSII particles with few Lhc antennas as compared with the more pure and intact C_2S_2M and $C_2S_2M_2$ complexes found in the B10 and B11 fractions.

In Vitro Aggregation—The addition of salts may be required in various experimental procedures, as for example in ion exchange chromatography. Grid preparation for electron microscopy may also require (optionally) the addition of some salt. Thus, we performed experiments to investigate the effect of salts on the solubility of PSII particles. The experiments were performed in a simple way (Fig. 4); we have observed the precipitation of $C_2S_2M_2$ particles in an Eppendorf tube after addi-

Downloaded from http://www.jbc.org/ by guest on June 19, 2019

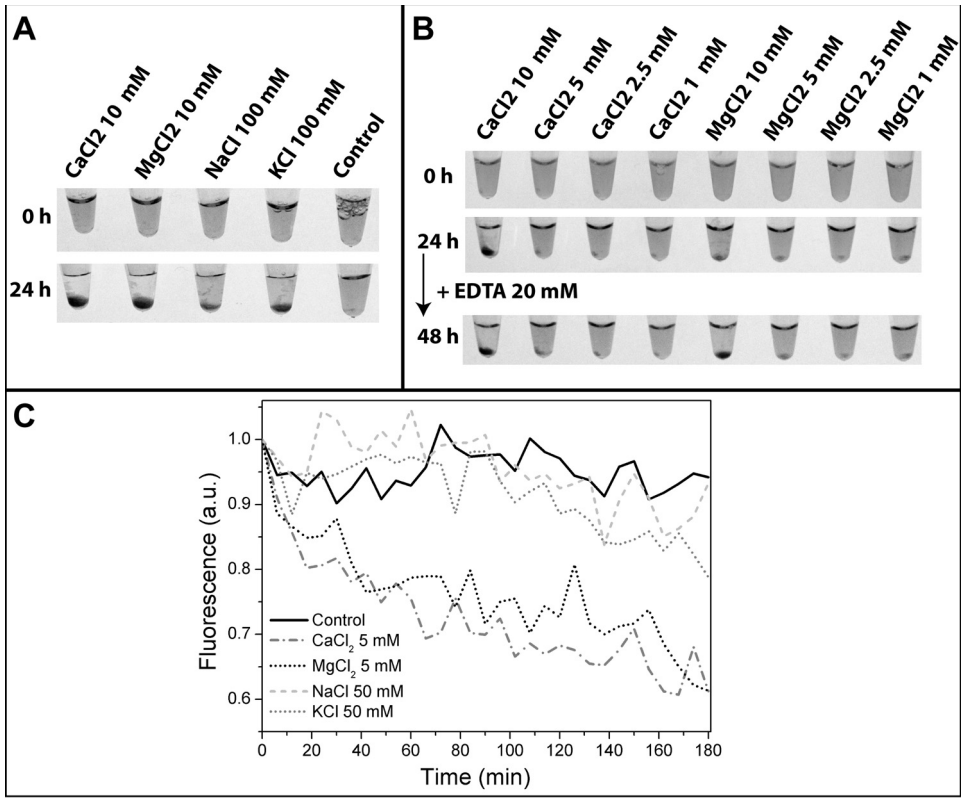


FIGURE 4. **Effect of ions on PSII aggregation.** *A,* purified PSII supercomplexes were incubated in the dark at room temperature in the presence of 10 mM $CaCl_2$ or $MgCl_2$ or 100 mM NaCl or KCl. A sample of purified PSII without additional ions was used as a control. Aggregation was visible by formation of a pellet after 24 h of incubation. *B,* same experiment was performed on ice at different concentrations of $CaCl_2$ and $MgCl_2$. Aggregation was visible in all tubes after 24 h. Pellets were resuspended in 20 mM EDTA and incubated for an additional 24 h in the ice. No reduction of the pellets was detected, and further aggregation was not prevented. *C,* fluorescence of the $C_2S_2M_2$ supercomplexes was measured every 6 min in presence of 5 mM $MgCl_2$, 5 mM $CaCl_2$, 50 mM NaCl, or 50 mM KCl for 3 h. The results are the average of three replicates and are normalized on the initial fluorescence. Average standard deviation for each curve was ~5%. The fluorescence is stable for the control (PSII particles without any added salt). NaCl was similar to the control. Addition of KCl induced a slow fluorescence decrease visible from 1.5 to 2 h of incubation, whereas $MgCl_2$ and $CaCl_2$ induced an immediate and significant fluorescence decrease, suggesting rapid aggregation of PSII particles.

tion of different amounts of monovalent (NaCl and KCl at 1, 10, 50, or 100 mM) and divalent ions ($MgCl_2$ and $CaCl_2$ at 1, 2.5, 5, or 10 mM). Divalent ions (as Mg^{2+}) showed a significant effect on PSII aggregation, even at low concentrations (5 mM). However, monovalent ions (such as Na^+) were also able to induce PSII aggregation over a longer period of time; after 24 h, aggregation could be observed in the samples containing 100 mM NaCl or KCl (Fig. 4*A*), as well as for lower concentrations, although the pellet was smaller (data not shown). In both cases, aggregation was induced at all temperatures tested, although aggregation occurred faster at room temperature than on ice (data not shown). Interestingly, addition of 20 mM EDTA to the tubes containing the divalent ions did not allow resolubilization and did not impede further aggregation (Fig. 4*B*). These results show that use of salts in buffers for experiments on PSII has a negative and irreversible effect on its solubility.

To determine whether these salts can be used for short incubations, we measured the fluorescence of the $C_2S_2M_2$ supercomplex for 3 h in presence of $MgCl_2$, $CaCl_2$, NaCl, and KCl at concentrations commonly used in experiments: 5 mM for divalent cations and 50 mM for monovalent cations, respectively (Fig. 4*C*). As for isolated antennas (32), some fluorescence quenching is expected in case of PSII aggregation, even if to a lower extent than for LHCII due to the much shorter excited state lifetime of PSII particles as compared with isolated antennas (see under "Time-resolved Fluorescence" below). In the control sample, without any addition of salts, the fluorescence is stable over the duration of the experiment, as was observed in the stability tests shown in Fig. 3. The addition of 50 mM NaCl did not affect the fluorescence on this time scale, suggesting that it can be safely used in buffers for short PSII incubations but not for long incubations as aggregation is visible at 24 h. 50 mM KCl induced a slow decrease of fluorescence after 1.5–2 h of incubation with PSII particles. Therefore, its use in buffers for experiments on PSII particles should be limited to shorter times. Addition of 5 mM $MgCl_2$ or $CaCl_2$, however, induced a very rapid and regular decrease of fluorescence, suggesting that their effect on PSII aggregation is immediate.

Low Temperature Steady-state Fluorescence—Fluorescence emission spectra of the four sucrose gradient fractions containing PSII particles with different antenna size, PSII dimeric core, purified trimeric LHCII, and grana membranes were measured at 77 K (Fig. 5). The fluorescence of LHCII showed a peak at 679.5 nm, whereas PSII core and supercomplexes had a maximum emission at 685 nm. All PSII supercomplexes showed very similar emission spectra, despite a very different antenna content, and B9, B10, and B11 spectra were virtually identical. These spectra look very similar to the emission spectrum of the isolated PSII dimeric core, indicating that at 77 K most of the energy is equilibrated on the PSII core.

Downloaded from http://www.jbc.org/ by guest on June 19, 2019

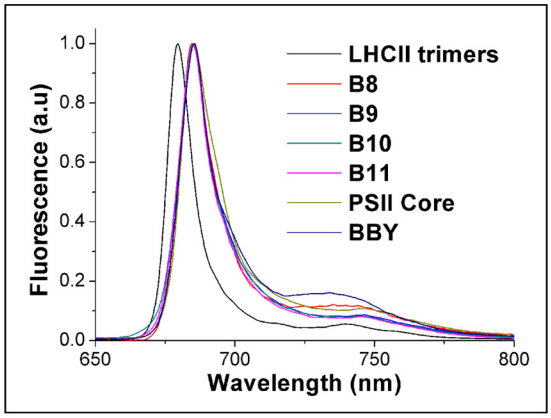


FIGURE 5. **Low temperature steady-state fluorescence emission of PSII supercomplexes.** Fluorescence emission at 77 K was measured for PSII supercomplexes in the B8 to B11 fractions, the purified LHCII trimers, the PSII dimeric core complex (12), and the grana membranes (BBY). The higher signal at ~735 nm for the BBY sample is due to a light contamination by PSI, which emits at ~735 m. Results were normalized on the peak of maximum fluorescence.

Time-resolved Fluorescence—The fluorescence decay kinetics of the $C_2S_2M_2$ particles were measured by time-correlated single-photon counting to investigate the functional integrity of PSII prepared in digitonin. Fig. 6*A* shows the decay of the excited state in $C_2S_2M_2$ supercomplexes obtained by monitoring the fluorescence at 680 nm, *i.e.* close to the room temperature emission maximum. The kinetics of excited state decay monitored in the 680–710-nm window are described by a sum of four exponentials characterized by lifetimes of 31, 164, and 571 ps and 1.9 ns. Fig. 6*B* shows the decay-associated spectra associated with each of these decay components. All the decay-associated spectra have similar band shapes, as observed previously for preparations of other PSII supercomplexes, as well as for the PSII-enriched BBY membranes. The amplitude associated with the longest living nanosecond component is less than 5%, and it is attributed, in accordance with a previous study (26), with a small fraction of closed PSII reaction centers. The remaining lifetimes in the sub-nanosecond range that describe the relaxation of open and photochemically active reaction centers are also in general agreement with those previously reported for the $C_2S_2M_2$ PSII supercomplex (26), albeit slightly slower. From these values, an average fluorescence lifetime τ_{av} of 210 ps is computed as shown in Equation 1,

$$\tau_{av} = \sum_i \alpha_i \tau_i \qquad \text{(Eq. 1)}$$

and is estimated as the mean value across the emission bandwidth, where α_i is the fractional amplitude of the component with lifetime τ_i. The maximal photochemical efficiency can be estimated from the relationship $\Phi_{PSII}^{max} = (\tau_m - \tau_{av})/\tau_m$, where τ_m is the average lifetime for closed reaction centers. Considering values of τ_m between 1.5 and 2.5 ns, Φ_{PSII}^{max} falls in the 0.86–0.89 interval. Thus, the analysis of time-resolved fluorescence lifetimes indicates that this novel PSII preparation is photochemically active and exhibits the expected trapping efficiency.

Detergent Screening—Determination of high resolution structural models of proteins and protein complexes is usually achieved by crystallization and interpretation of the x-ray diffraction pattern. Alternative approaches are electron microscopy on two-dimensional crystals (33) or on single particles (34). In the case of membrane proteins, the use of one or more detergents is necessary to avoid protein aggregation, but the presence of detergents can reduce the chance of crystallization or even cause protein denaturation or complex disassembly. This constraint is one of the most important issues that have limited the number of successfully crystallized membrane proteins. In the case of plant PSII, indeed the crystal and its structure have not yet been obtained.

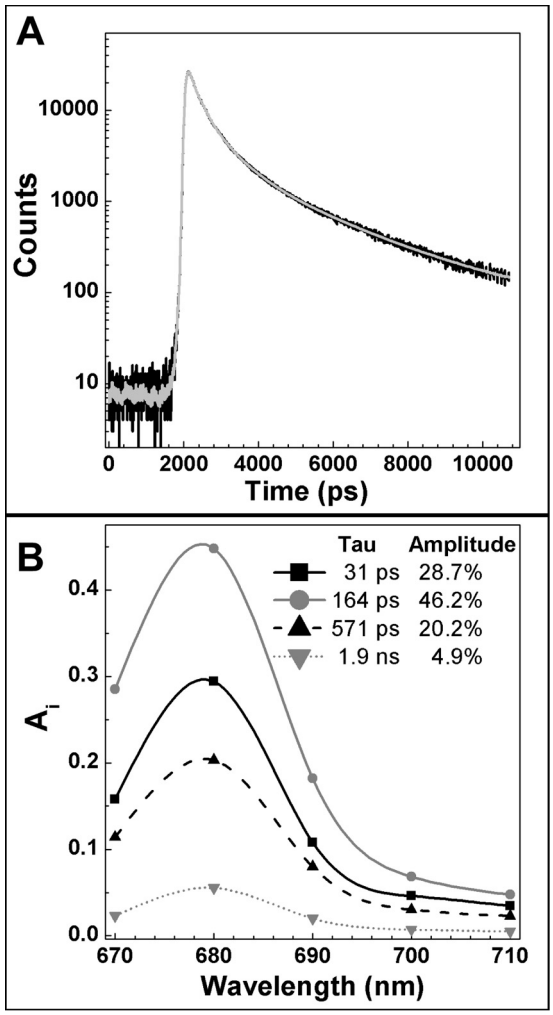


FIGURE 6. **Time-resolved fluorescence measurements.** *A,* excited state decay kinetics of purified $C_2S_2M_2$ particles (fraction B11) was monitored by time-correlated single photo counting fluorescence technique (*black trace*) and fit with an exponential function (*gray trace*). *B,* four components were retrieved by global fitting. The decay-associated spectra and the values for the lifetimes (τ) and the amplitudes are indicated in figure.

To test which detergents might be suitable for crystallization trials on PSII, we performed a stability test of our digitonin preparation by adding a large number of classical detergents used in crystallization (digitonin is not a classical detergent for this application). The change in the fluorescence signal was an indicator of the supercomplex stability, as described under "PSII Stability." Because of the large number of detergents screened, we traced fluorescence changes with a quantitative RT-PCR machine that has suitable excitation lights and emission filters for chlorophyll fluorescence detection, and we also

Downloaded from http://www.jbc.org/ by guest on June 19, 2019

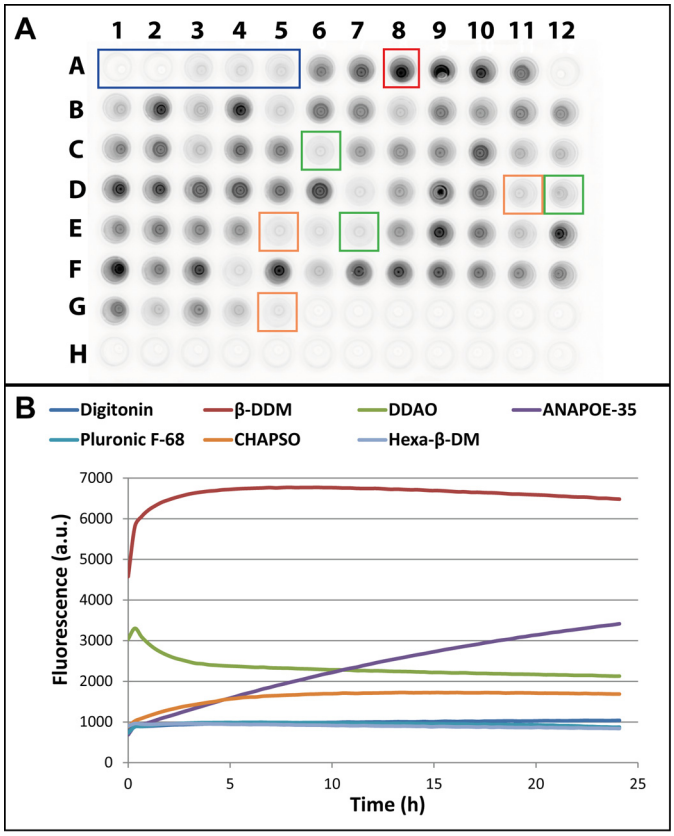


FIGURE 7. **Detergent screen for PSII stability.** *A,* PSII stability has been tested in the presence of 73 detergents (full list in supplemental Table 1). These detergents were individually added to digitonin-purified $C_2S_2M_2$ particles at a concentration of 1.5× CMC. A picture of the plate was taken at the end of the incubation. Controls are *framed* in *blue* (from *left to right*: 2 wells with only buffer, 2 wells with PSII without any additional detergent, and 1 well with PSII and additional digitonin). β-DDM, a detergent known for degrading PSII supercomplexes, is *framed* in *red*. *Orange boxes* show detergents maintaining PSII structure but not further tested (CHAPS, C-HEGA®-8 and CYMAL®-1). *Green boxes* show detergents (Pluronic F68, CHAPSO, and *n*-hexadecyl-β-D-maltoside) further tested for PSII purification (Fig. 8). *B,* fluorescence in the plate in *A* was measured every 20 min for 24 h. The different types of results are shown here: the three selected detergents (Pluronic F68, CHAPSO, and Hexa-β-DM), like digitonin, induce low fluorescence increase during the incubation. β-DDM (*A8* in *A*) shows a fast and important increase of the fluorescence, indicating immediate sample degradation. A similar degradation was observed with ANAPOE-35 (*C7*), although it was much slower. Finally, some detergents, like DDAO (*B8*), showed an initial increase of fluorescence, then a decrease, suggesting initial degradation followed by aggregation of the sample.

measured the final fluorescence signal by a video-imaging system (see "Experimental Procedures" for details).

Each detergent was added to a final concentration of 1.5× CMC (from a stock 10× CMC), and the fluorescence was followed during 24 h at room temperature. The final picture is shown in Fig. 7*A*. β-DDM detaches at least part of the antenna system and was used as a sort of positive control for supercomplex disassembly. α-DDM is absent from this plate, but as expected (see above and Ref. 12), it showed a similar result in a second experiment (data not shown). PSII with no detergent added or in digitonin 1.5× CMC was the negative control, as PSII is stable in these conditions over a long period. The screening of about 70 detergents (full list in supplemental Table 1) showed that most of the detergents are unable to maintain PSII integrity, each one having a different effect on the rate of PSII disassembly. It should be noted that some wells containing detergents not selected for further analysis appear clear, suggesting a low fluorescence. They correspond to detergents that induced an initial rise of fluorescence, then an important diminution during the 24-h kinetic experiment (Fig. 7*B*). Unfortunately for structural purposes, detergents commonly used for crystallization such as α- and β-DDM, or the newer lauryl-maltose neopentyl-glycol (35), destabilize the PSII structure quite rapidly.

A few detergents (CHAPS, CHAPSO, *n*-hexadecyl-β-D-maltoside, C-HEGA8, Pluronic F68, and CYMAL1) showed a small increase in the fluorescence signal indicating a very small effect on PSII stability at this concentration. These detergents were tested again at 5× CMC concentrations (data not shown) and all, but the CHAPS, showed again a small fluorescence increase indicating that PSII likely remains assembled in these conditions.

Pluronic F68, CHAPSO, and *n*-hexadecyl-β-D-maltoside were further tested for their suitability in membrane solubilization and gradient fractionation to see whether the entire PSII preparation could be performed with these detergents. C-HEGA8 and CYMAL1, which have a very high CMC (277 and 340 mM, respectively), were not further tested.

First, different concentrations of the three selected detergents were used to solubilize grana membranes. We found that only hexa-β-DM was efficient, mostly at the highest concentration (0.8%, corresponding to its solubility limit), although the amount of membrane solubilized was low compared with the protocols using α-DDM (12) or digitonin (Fig. 8*A*). Next, α-DDM/digitonin-solubilized membranes were loaded on gradients containing the three selected detergents (0.5 and 0.05% in the case of Pluronic F68 and CHAPSO; 0.0003 and 0.00003% for hexa-β-DM, which correspond to 10× CMC and CMC). Only CHAPSO and hexa-β-DM gradients showed normal separation profiles (with slightly better results at the lowest concentrations) (Fig. 8*B*).

As hexa-β-DM was also able to solubilize BBY, the supernatant containing the solubilized PSII particles was also loaded on gradients containing either 0.01% digitonin or 0.00003% hexa-β-DM (Fig. 8*C*). The bands obtained on these gradients were not as clearly defined as they were after a standard digitonin/α-DDM solubilization, and the yield was also lower; $A_{680\ nm}$ was about 0.2, which is about 3–4 times lower than typically obtained for the standard protocol in similar conditions. In both cases, however, the spectrum obtained for the most abundant band in the supercomplexes was very similar to the one obtained for $C_2S_2M_2$ purified in α-DDM and digitonin (Fig. 8*D*), suggesting that the complete purification of PSII can be performed in hexa-β-DM if needed.

PSII stability after purification in CHAPSO or in hexa-β-DM was also tested (Fig. 8, *E* and *F*). The results show that in all conditions, the purified PSII is functional, as shown by the diminution in fluorescence after addition of ferricyanide, which attests to the presence of an electron transfer and a connected antenna system. PSII is very stable (as proven by a low and constant fluorescence signal) when purified in hexa-β-DM or in 0.05% CHAPSO. In 0.5% CHAPSO, however, the complexes showed a more important initial fluorescence, which increased

Downloaded from http://www.jbc.org/ by guest on June 19, 2019

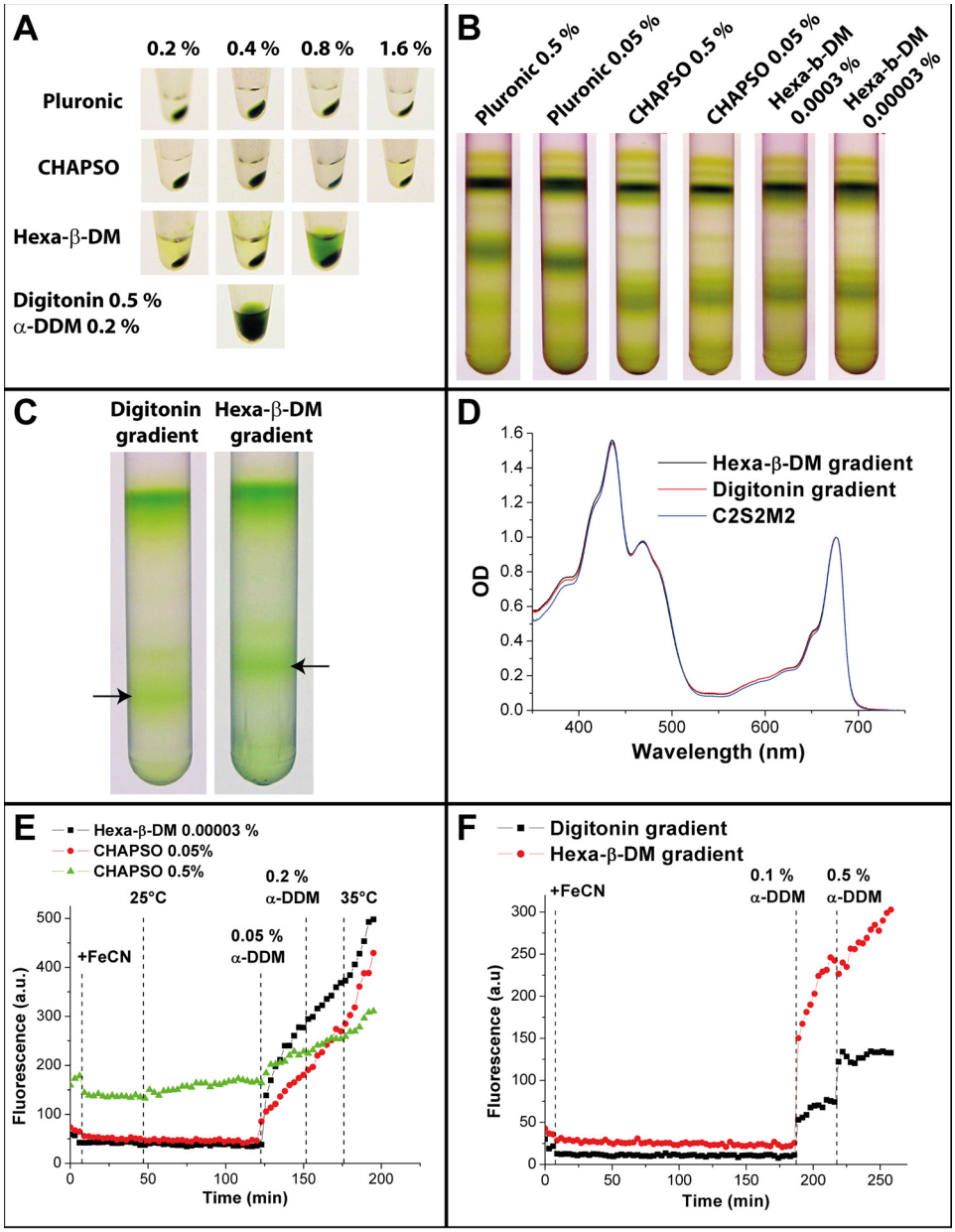


FIGURE 8. **PSII purification in selected detergents.** *A,* BBY membranes were solubilized with increasing concentrations of Pluronic F68, CHAPSO, and hexa-β-DM and centrifuged at 12,000 × *g* for 10 min. Solubilized supercomplexes were in the supernatant. Membranes solubilized in 0.5% digitonin, 0.2% α-DDM were used as a control. *B,* BBY membranes solubilized in digitonin and α-DDM were deposited on sucrose gradients containing different concentrations of Pluronic F68, CHAPSO or hexa-β-DM. Gradients performed in Pluronic F68 showed a degradation of the PSII supercomplex. Gradients in CHAPSO and hexa-β-DM had similar profiles as compared with digitonin gradients. *C,* BBY membranes solubilized in 0.8% hexa-β-DM were separated on sucrose gradients containing either 0.01% digitonin or 0.00003% hexa-β-DM. PSII supercomplexes could be purified from both gradients (*arrows*). *D,* absorption spectra of the supercomplexes purified from the gradients in *C*, normalized in the *red region*. The spectra are almost identical and correspond well to a $C_2S_2M_2$ spectrum. *E,* stability of the $C_2S_2M_2$ supercomplexes purified in gradients shown in *B*. Supercomplexes were incubated at 5 °C. 0.3 mM ferricyanide was added after the third measure. After about 40 min, temperature was increased to 25 °C. After about 1.5 and 2.5 h, the PSII was degraded by addition of α-DDM and finally by increasing the temperature to 35 °C. *F,* similar stability test at room temperature on PSII supercomplexes purified in gradients from *C*. Both samples are stable for at least 3 h at room temperature.

slightly if the PSII was left at room temperature, showing that, at this concentration, CHAPSO induces some degradation of the supercomplex. In conclusion, we identified some detergents that could preserve PSII integrity and thus could be used for biochemical experiments and crystallization assays.

Discussion

In this work, we present an improved protocol for the preparation of PSII particles with different antenna sizes whose stability is much increased with respect to a previous preparation (12). A biochemical and spectroscopic characterization was also performed to complement data previously obtained on similar but less stable particles. The use of the very soft digitonin detergent has been fundamental for the stabilization of the weak subunit interactions in the PSII supercomplex. This is similar to the case of the PSI-LHCII supercomplex (27), which was purified in a similar manner and which is unstable in α-DDM. Very likely, the use of the large and bulky digitonin

Downloaded from http://www.jbc.org/ by guest on June 19, 2019

allows maintaining the weak interactions between subunits, especially at the level of the antenna system. However, when α-DDM is added, which is also a mild detergent but smaller and with a long aliphatic chain, the weak connections are disrupted.

We showed that ions can induce aggregation of the PSII particles, especially in the case of divalent ions such as Mg^{2+}. It is likely that the ions mask the charges on the surfaces of Lhc proteins, especially LHCII (36), promote interactions, and finally aggregate the PSII in solution. Similar interactions between stromal PSII surfaces are present in a more ordered way *in vivo* and are fundamental for maintaining the stacking of the grana membranes. It is thus preferable to avoid salts in buffers used for experiments on PSII, especially divalent cations, such as $MgCl_2$ and $CaCl_2$, which induce immediate aggregation. NaCl and KCl, which only affect PSII particles after a longer time, may likely be used for short incubation times (Fig. 4).

The PSII supercomplexes purified with this protocol also retain a larger quantity of the peripheral PsbP subunit than the α-DDM preparation. PsbQ is also present in the supercomplexes in similar proportion as compared with the leaves. PsbR as well seems to be entirely retained in the purified particles, although the study of its stoichiometry by densitometry on gel showed that it was in substoichiometric amount as compared with PsbE, an essential and integral subunit of the PSII core (Fig. 2*B*). Similarly, both PsbP and PsbQ are scarcely visible on gels (Fig. 1*C*); PsbP has a lower intensity than subunits with a similar molecular weight present in 1:1 stoichiometric amounts with the core as CP24 or Lhcb3; PsbQ, which has a mass of about 17 kDa, is also barely visible in PSII fractions and BBY membranes. Thus, it is possible that these proteins are present in variable amounts and were not in stoichiometric quantity in our leaves. Indeed, it has already been suggested that PsbP might be essential for seedlings but is dispensable in older leaves, in which its level decreases (37). In contrast, it has been suggested that these proteins, and especially PsbP, are important for maintenance of calcium and chloride in the oxygen-evolving complex (38).

However, it should be noted that PsbP and PsbQ loss has been detected in almost all PSII preparations published so far, which has been mainly core preparation in the 1980s (39) or PSII-LHCII supercomplexes more recently (12, 20, 25, 28). It can be noted that, in the three-dimensional structure of the C_2S_2 supercomplex from spinach recently obtained by Wei *et al.* (25), both PsbP and PsbQ densities are weak and visible only when the three-dimensional volume visualization is decreased to a very low level (at which a lot of noise appears), which suggests their substoichiometric amount in purified PSII particles. However, it is possible that these subunits are more tightly bound to the core in spinach than in *Arabidopsis*. Such a difference between plant species has indeed already been suggested (40). It should also be noted that in the recent three-dimensional structure of the C_2S_2 supercomplex (25), PsbR was not identified. However, in this work the presence of PsbR in the purified PSII was not investigated. The apparent low amount of peripheral subunits can also suggest that PSII complexes *in vivo* might be heterogeneous. Thus, the role and stoichiometry of these proteins require further investigation.

Interestingly, we also showed that the pH of the buffer has some effect on the association of PsbP, whose binding to PSII is stronger at low pH. Considering that during the photosynthetic process the luminal pH decreases, it cannot be excluded that this has a physiological significance. Indeed, it has already been proposed that the PsbP role in maintaining the Ca^{2+} binding at the water-oxidizing site might be particularly important at acidic pH (40).

O_2 evolution experiments on our BBY preparation and PSII particles show that PSII is active. Our grana membrane preparation showed an activity similar to that of the original spinach BBY preparation (~270 *versus* ~300 μmol of O_2·mg(Chls)$^{-1}$·h^{-1}, respectively) (41). O_2 evolutions in Ref. 41 were similar at pH 6 and 7 and decreased only at pH 8. The same PSII activity was obtained by Kuwabara and Murata (42), who also showed a significant decrease for pH >7.8 and a rather constant activity in a range of pH 6.8–7.3.

Several other papers reported similar PSII activities (43, 44) but also different values depending on the plant species/genotype and on the addition of Ca^+ and/or Cl^- in the buffer. In particular, Enami *et al.* (44), using similar conditions as in our work, obtained on spinach a value of ~400 μmol of O_2·mg(Chls)$^{-1}$·h^{-1}, increased to 475 μmol of O_2·mg(Chls)$^{-1}$·h^{-1} in the presence of Ca^+ and to ~640 μmol of O_2·mg(Chls)$^{-1}$·h^{-1} in the presence of a different electron acceptor (phenyl-*p*-benzoquinone). Higher O_2 evolution rates were found using membranes from mutant plants with a very low antenna content: Shen *et al.* (39) measured a value of 860 μmol of O_2·mg(Chls)$^{-1}$·h^{-1} on BBY strongly depleted of LHCII. However, by considering that normal BBY have ~240 Chls per reaction center, and membrane from the mutant only ~53 Chls (39), the "normalized" (to comparable amounts of reaction center) O_2 evolution for BBY depleted in LHCII is ~200 μmol of O_2·mg(Chls)$^{-1}$·h^{-1}. In this work, loss of PsbP and PsbQ subunits was also detected during membrane preparation, and O_2 evolution was improved by subsequent addition of these subunits or addition of Cl^-.

Concerning activity of purified PSII complexes, most of the reports are on PSII core preparations or PSII strongly deprived of LHCII, because a purification of homogeneous and intact PSII particles had always been difficult. PSII core complexes (or with low antenna content) showed values at 1000–1300 μmol of O_2·mg(Chls)$^{-1}$·h^{-1} (39). By considering that our $C_2S_2M_2$ particle contains ~160 Chls per reaction center, and PSII core complexes only 35 Chls, the normalized O_2 evolution for the latter is ~210–280 μmol of O_2·mg(Chls)$^{-1}$·h^{-1}. Our PSII preparation has therefore an activity slightly lower (180 μmol of O_2·mg(Chls)$^{-1}$·h^{-1}) than other preparations, but higher than the 75 μmol of O_2·mg(Chls)$^{-1}$·h^{-1} measured on the smaller C_2S_2 supercomplex recently resolved by cryo-EM (25). Despite the low amount of some peripheral subunits, however, steady-state and time-resolved fluorescence showed that the PSII particles are energetically well connected. In particular, the low temperature fluorescence spectra of all particles from B8 (C_2S and C_2M) to B11 ($C_2S_2M_2$) corresponded well to those obtained from the isolated dimeric core of PSII. These data show that, no matter the antenna size of the PSII, the energy is equilibrated on the core, which accounts for only ~22% of the

Downloaded from http://www.jbc.org/ by guest on June 19, 2019

total Chl content in the case of largest $C_2S_2M_2$ supercomplex (11).

Time-resolved fluorescence analysis proved that the largest purifiable $C_2S_2M_2$ PSII supercomplex is energetically connected and photochemically active, and the quantum conversion efficiency is comparable with those obtained from previous purifications of PSII supercomplexes having analogous antenna dimensions (12). The PSII particles purified are thus not only stable but they remain functional over time and after freezing and thawing.

Our particles are thus suitable for investigation on PSII energy transfer properties, although improvements for O_2 evolution activity are likely still possible. For instance, use of 2 M glycine betaine seems effective in maintaining a higher amount of PsbP and PsbQ bound to PSII (45).

We also showed by pigment analysis that, for the largest $C_2S_2M_2$ particle, pigments contribute to more than 20% of its molecular mass (1500 kDa) and in particular of ~312 total Chls, ~100 of which are Chls *b*. The complex also binds ~85 Cars in total; around 43 luteins, ~14 neoxanthins, and ~7 violaxanthins are bound to the Lhc antenna system; the remaining carotenoids (~22 β-carotenes) are bound to the core complex. The $C_2S_2M_2$ supercomplex contains a total of 12 LHCII monomers and nine monomeric Lhc. Site N1 is absent only in CP24 (46), thus, a value of 14 neoxanthin molecules corresponds to an almost complete occupancy of the N1 site in the other Lhc complexes. On the contrary, the content of violaxanthin, which is mainly bound to the V1 site of LHCII (47, 48), but also in Lhc internal sites, is low; our results show that violaxanthin is significantly less abundant in *Arabidopsis* as compared with spinach or maize (11). Thus, the peripheral site V1 of LHCII, which is occupied mainly by violaxanthin in maize (48) or spinach (49), is occupied mainly by lutein in *Arabidopsis*.

We also investigated the effect of several common detergents on PSII stability, in order to identify those that could be used for further structural studies of the complex, such as crystallization. Digitonin is indeed usually not used for this purpose (50), although it has already been used for solubilization of complexes before crystallization (51). We found that most of the detergents tested have a detrimental effect on PSII integrity, strongly reducing the choice of detergents suitable for use with PSII. Indeed, the preparation of pure and stable plant PSII particles is made difficult by the weak binding of some of its subunits, especially the external antenna system. Two of the tested detergents, however, permitted the purification of $C_2S_2M_2$ particles, CHAPSO and *n*-hexadecyl-β-D-maltoside. It is interesting to note that CHAPSO has already been used for crystallization experiments (52–54). It could thus represent an interesting alternative to α-DDM and digitonin for such structural experiments. However, in contrast to hexa-β-DM, it can be used only for fractionation on gradients and to some extent conservation of the particles but not for solubilization of the membranes. Indeed, complete purification of $C_2S_2M_2$ could also be performed in hexa-β-DM, although the yield is lower and the supercomplexes are probably less pure than after purification in digitonin and α-DDM, as the bands in the gradient were less defined.

In conclusion, the new protocol presented here allows an easy preparation of stable PSII particles that do not disassemble even when held at temperatures above room temperature for several hours/days. Moreover the particles can be concentrated up to ~6 mg/ml (and likely even more), which correspond to an $A_{680\ nm}$ ~80 cm^{-1}. Such preparations are therefore suitable for several kinds of functional and structural experiments that require high protein concentration, such as time-resolved absorption spectroscopy (performed usually in a cuvette with a very short path length) and cryo-electron microscopy.

To our knowledge, this new plant PSII preparation is the most stable as published so far. In this work we used *Arabidopsis*, because it is the most utilized model organism in plant biology and for which several mutants exist. However, the same protocol can be applied to other species (we obtained the same results, here not shown, on maize). Our work will thus open new possible approaches to investigate plant and algae photosystem II operation.

Experimental Procedures

Standard Preparation and Low pH Preparations—PSII-enriched membranes (BBY) were prepared from *A. thaliana* WT Col0 plants, following the same protocol as in Ref. 12.

PSII supercomplexes were fractioned from these membranes on a sucrose gradient containing 0.35 M sucrose, 10 mM Hepes-KOH, pH 7.5, and 0.01% w/v digitonin. Gradients were formed by freezing and thawing. 200 μg (in chlorophylls) of BBY membranes were washed with 10 mM Hepes-KOH, pH 7.5, then resuspended at a concentration of 1 mg/ml in 10 mM Hepes-KOH, pH 7.5, and solubilized by adding an equal volume of 1% w/v digitonin and 0.4% w/v α-dodecylmaltoside to have a final chlorophyll concentration of 0.5 mg/ml and a final detergent concentration of 0.5% digitonin and 0.2% α-DDM. The samples were incubated on ice in the dark for 30 min, then centrifuged at 12,000 × *g* for 10 min to eliminate unsolubilized material, and deposited on the gradients. Ultracentrifugation was performed on an SW41 rotor at 41,000 rpm for 7 h or on an SW60 rotor at 60,000 rpm for 2.5 h (in this case, 100 μg of chlorophylls per gradient were used). For overnight centrifugation, a similar separation was obtained by centrifuging for 17 h at 41,000 rpm in an SW41 rotor using a gradient obtained with an initial concentration of 0.65 M sucrose.

For the low pH preparations, a similar protocol was used by replacing Hepes with 10 mM MES at a pH of either 6.5 or 6. Detergent concentration was also increased during the membrane solubilization, to reach a total of 0.5% digitonin and 0.25% α-DDM for pH 6.5 and 0.5% digitonin and 0.3% α-DDM for pH 6.

Membrane solubilization in presence of Pluronic F68, CHAPSO, and hexa-β-DM was performed in a similar manner as described above, except digitonin and α-DDM were replaced by the detergent of interest at a final concentration of 0.2, 0.4, 0.8, or 1.6% (CHAPSO and Pluronic F68 only). In the case of 0.8% hexa-β-DM, the pelleted membranes were resuspended in the detergent without prior addition of buffer.

For separation on Pluronic F68, CHAPSO, and hexa-β-DM gradients, BBY membranes solubilized in digitonin and α-DDM were deposited on sucrose gradients containing 0.5 or

Downloaded from http://www.jbc.org/ by guest on June 19, 2019

0.05% of Pluronic F68 or CHAPSO or 0.0003 and 0.00003% of hexa-β-DM. For gradient fractionation with hexa-β-DM, solubilization with 0.8% hexa-β-DM was performed, and the samples were deposited on gradients containing 0.35 M sucrose, 10 mM Hepes-KOH, pH 7.5, and either digitonin 0.01% or hexa-β-DM 0.00003%, which corresponds to the CMC. Ultracentrifugation was made in an SW41 rotor, at 41,000 rpm for 7 h.

Steady-state Fluorescence—Fluorescence emission spectra were measured at 77 K with a Cary Eclipse fluorimeter for gradient fractions containing PSII particles with different antenna size, PSII dimeric core, purified trimeric LHCII, and BBY membranes. Excitation was made at 440 nm with a 10 nm bandwidth, and emission was measured between 600 and 800 nm with a 0.5-nm step.

Time-correlated Single Photon Counting Fluorescence Measurements—The excited state decay kinetics were monitored in a laboratory assembled setup, previously described in detail (55). In brief, the sample was excited at 632 nm (full width at half-maximum 3 nm) with a pulsed diode laser (PicoQuant 800B) at a repetition rate of 20 MHz. The excitation intensity is sufficiently low (20 pJ/pulse) to avoid the occurrence of nonlinear processes. The emitted photons are collected at right-angle geometry, at magic angle polarization, by a cooled multichannel plate photomultiplier (Hamamatsu, R5916U-51). The emission wavelength was selected with a monochromator (Jasco JT-10). The photons' time of arrival distribution was detected with a time-to-amplitude converter, constant fraction discriminator, and stored in multichannel storage devices integrated in a computer card (Becker & Hinkl, SPC-330).

The instrument response function, as determined using the reference dye pinacyanol, is 110 ps. This allows resolving lifetimes, which are an order of magnitude faster after numerical deconvolution of the instrumental response.

The data were analyzed with a laboratory-developed software (56) using the global iterative reconvolution methods, considering the measured instrument response and a model decay function consisting of a sum of weighted exponentials. The results of the fit are the wavelength-independent lifetimes (τ) and the (wavelength-dependent) weighting amplitudes ($A_i(\lambda)$). The plot of the amplitude as a function of the emission wavelengths yields the decay associated spectra. The value of the effective trapping constant K_{tr} is approximated to the inverse of the average decay lifetime, which is determined from the fitted parameters as shown in Equation 2,

$$\tau_{av} = \sum_i A_i\tau_i / \sum_i A_i \qquad \text{(Eq. 2)}$$

For the measurements, the sample was held in a 3-mm path length cuvette, at an optical density of 0.1 cm^{-1} at the maximal absorption in a buffer containing 0.7 M sucrose, 10 mM Hepes, pH 7.5, 0.015% digitonin, and in the presence of 25 μM dichlorophenolindophenol and 500 μM ferricyanide.

HPLC—Pigments from PSII particles with different antenna sizes (B8 to B11 on the sucrose gradients) and purified LHCII were extracted in 80% acetone at a final $A_{680\ nm}$ of 0.4 cm^{-1}, and their pigment content was analyzed by absorption spectroscopy (57) and HPLC (58). Pigments were separated according to their hydrophobicity on a C18 column.

Stability Test—PSII stability was tested by measurement of fluorescence changes under different conditions (similarly as in Ref. 12), as detachment of LHCII antennas from PSII results in an increase in fluorescence. Fluorescence emission of $C_2S_2M_2$ supercomplexes at an $A_{680\ nm}$ of 0.05 cm^{-1} was measured with a Cary Eclipse fluorimeter at 680 nm upon excitation at 590 nm (5 nm bandwidth) filtered with a 3% T filter. 0.3 mM ferricyanide was added after the third time point (each point every 3 min). For the stability test at high temperature, temperature was gradually increased from 5 to 35 °C. For the other tests, it was maintained at 22 °C, although digitonin (up to 0.4%) or NaCl concentrations (up to 0.5 M) were gradually increased. At the end of each experiment, 0.1% α-DDM was added to induce disassembly of the supercomplex.

For stability tests of supercomplexes purified in CHAPSO or hexa-β-DM gradients, the supercomplexes were first incubated at 5 °C. After about 40 min, the temperature was increased to 25 °C. After addition of α-DDM (0.05%, then to a final concentration of 0.2%), the PSII was further degraded by increasing the temperature to 35 °C.

Oxygen Evolution—O_2 production was measured in a Clark-type oxygen electrode system on BBY membranes concentrated 10 μg/ml (in Chls) in 0.4 M sorbitol, 15 mM NaCl, 5 mM $MgCl_2$, 10 mM Hepes-KOH, pH 7.5, and on $C_2S_2M_2$ particles at 10 μg/ml (in Chls) in 0.6 M sucrose, 0.01% digitonin, 10 mM Hepes-KOH, pH 7.5, at 20 °C using 5000 μmol of photons·m^{-2}·s^{-1} of white light. 0.15 mM ferricyanide and 0.1 mM dichlorobenzoquinone were then added as electron acceptors.

Detergent Screening—PSII stability was further tested in the presence of 73 detergents (full list in supplemental Table 1). For the screening, these detergents were individually added to $C_2S_2M_2$ supercomplexes prepared in digitonin (as described above) at an $A_{680\ nm}$ of 0.15 cm^{-1} in presence of 0.3 mM ferricyanide in a 96-well plate. Detergent concentration was adjusted to 1.5× CMC from a stock at 10 CMC. To detect PSII degradation, fluorescence was measured every 20 min for 24 h in a RT-PCR machine (CFX96 Touch, Bio-Rad) with filters designed for a Cy5 fluorophore, which are also appropriate for chlorophylls (excitation 620–650 nm and emission 675–690 nm). At the end of the incubation, a picture of the plate was taken in a video-imaging system (Fusion FX7, Vilbert-Lourmat).

SDS-PAGE and Immunoblot Analyses—Gradient fractions were separated on a SDS-polyacrylamide gel (59) with a 14% concentration of acrylamide/bisacrylamide 29:1 and 2 M urea. The gel was loaded with different volumes of the fractions, normalized to correspond to 0.15 μg of chlorophylls for LHCII (B3 fraction). The coefficients applied to the $A_{680\ nm}$ to determine the volume were as follows: B1, 30; B2, 18; B3, 20; B4, 16; B6, 7.2; B7, 6.27; B8, 6.82; B9, 7.14; B10, 7.39; B11, 7.62.

For PsbS analysis, the fractions were separated on Laemmli SDS-PAGE with 14% acrylamide/bisacrylamide 29:1 and 6 M urea, which allows separating PsbS and CP24 bands. The gels were loaded with 0.15 μg of chlorophylls for LHCII.

For PsbR analysis, a B11 band was deposited on a Tris-Tricine (60) gel with 16% acrylamide/bisacrylamide 29:1. PsbR identity (~10.2 kDa) was confirmed by immunoblot. PsbE

Downloaded from http://www.jbc.org/ by guest on June 19, 2019

assignment is based on its mass (~9.4 kDa), considering that the next low molecular subunit, PsbH, has a much lower mass (~7.7 kDa). All gels were stained with Sypro Ruby.

Immunoblots were performed with anti-PsbO, anti-PsbP, anti-PsbQ, anti-Lhcb4, anti-Lhcb6 (lots 0512, 0702, 1101, 0601 and 0712, respectively), and anti-PsbR antibodies (all from Agrisera). PsbS antibody was raised in rabbit against the synthetic (C)-TGKGALAQFDIETG peptide. This sequence (corresponding to the first part of the second luminal loop of PsbS) has been chosen for the good predicted antigenicity and for the strong conservation between PsbS proteins of many green organisms to have a wide cross-reactivity. The antibody was tested and characterized in Ref. 61. Chemiluminescent detection was performed using a Fusion FX7 detection system (Vilbert-Lourmat). Quantification was made by densitometry.

Aggregation Experiments—$C_2S_2M_2$ supercomplexes were concentrated to an $A_{680\,nm}$ of about 4 cm^{-1} and incubated in the dark at room temperature or on ice, in the presence of $CaCl_2$ or $MgCl_2$ (concentrations tested: 1, 2.5, 5, and 10 mM) and NaCl or KCl (1, 10, 50, and 100 mM). Aggregation was checked visually (formation of a pellet) after 24 h. After the experiment on ice, the pellet of all tubes containing divalent ions was resuspended with 20 mM EDTA and incubated in the same conditions for another 24 h.

Aggregation kinetics experiments were performed by measure of fluorescence emission of $C_2S_2M_2$ particles at an $A_{680\,nm}$ of 0.1 cm^{-1} in the presence of 0.3 mM ferricyanide in a Cary Eclipse fluorimeter at 680 nm upon excitation at 590 nm (5 nm bandwidth) filtered with a 3% T filter. Fluorescence was measured every 6 min for 3 h. The results are normalized on the initial fluorescence of the sample, and are the average of three replicates.

Author Contributions—S. C. designed the study. A. C. performed the experiments. S. S. performed the time-resolved fluorescence experiment. S. C., A. C., and S. S. wrote the paper. All authors analyzed the results and approved the final version of the manuscript.

Acknowledgments—We thank Fabrice Richard and Aïcha Aouane (Institut de Biologie du Développement de Marseille (IBDM)) for technical help with electron microscopy. Pascal Arnoux (Laboratoire de Bioénerétique Cellulaire (LBC)) is thanked for providing the detergent kit. Ben Field (Laboratoire de Génétique et Biophysique des Plantes) is thanked for manuscript revision. Electron microscopy work was supported by the French National Research Agency through the "Investments for the Future" program (France-BioImaging, ANR-10-INSB-04) and was performed at the PiCSL-FBI core facility (Institut de Biologie du Développement de Marseille, AMU-Marseille UMR 7288).

References

1. Hohmann-Marriott, M. F., and Blankenship, R. E. (2011) Evolution of photosynthesis. *Annu. Rev. Plant. Biol.* **62,** 515–548
2. Adir, N. (2005) Elucidation of the molecular structures of components of the phycobilisome: reconstructing a giant. *Photosynth. Res.* **85,** 15–32
3. Shi, L. X., and Schröder, W. P. (2004) The low molecular mass subunits of the photosynthetic supracomplex, photosystem II. *Biochim Biophys Acta* **1608,** 75–96
4. Roose, J. L., Wegener, K. M., and Pakrasi, H. B. (2007) The extrinsic proteins of photosystem II. *Photosynth. Res.* **92,** 369–387
5. Bricker, T. M., Roose, J. L., Fagerlund, R. D., Frankel, L. K., and Eaton-Rye, J. J. (2012) The extrinsic proteins of photosystem II. *Biochim. Biophys. Acta* **1817,** 121–142
6. Ifuku, K., and Noguchi, T. (2016) Structural coupling of extrinsic proteins with the oxygen-evolving center in photosystem II. *Front. Plant Sci.* **7,** 84
7. García-Cerdán, J. G., Kovács, L., Tóth, T., Kereïche, S., Aseeva, E., Boekema, E. J., Mamedov, F., Funk, C., and Schröder, W. P. (2011) The PsbW protein stabilizes the supramolecular organization of photosystem II in higher plants. *Plant J.* **65,** 368–381
8. Loll, B., Kern, J., Saenger, W., Zouni, A., and Biesiadka, J. (2005) Towards complete cofactor arrangement in the 3.0 angstrom resolution structure of photosystem II. *Nature* **438,** 1040–1044
9. Guskov, A., Kern, J., Gabdulkhakov, A., Broser, M., Zouni, A., and Saenger, W. (2009) Cyanobacterial photosystem II at 2.9-A resolution and the role of quinones, lipids, channels and chloride. *Nat. Struct. Mol. Biol.* **16,** 334–342
10. Umena, Y., Kawakami, K., Shen, J. R., and Kamiya, N. (2011) Crystal structure of oxygen-evolving photosystem II at a resolution of 1.9 A. *Nature* **473,** 55–60
11. Caffarri, S., Tibiletti, T., Jennings, R. C., and Santabarbara, S. (2014) A comparison between plant photosystem I and photosystem II architecture and functioning. *Curr. Protein Pept. Sci.* **15,** 296–331
12. Caffarri, S., Kouril, R., Kereïche, S., Boekema, E. J., and Croce, R. (2009) Functional architecture of higher plant photosystem II supercomplexes. *EMBO J.* **28,** 3052–3063
13. Dekker, J. P., and Boekema, E. J. (2005) Supramolecular organization of thylakoid membrane proteins in green plants. *Biochim. Biophys. Acta* **1706,** 12–39
14. Ballottari, M., Girardon, J., Dall'osto, L., and Bassi, R. (2012) Evolution and functional properties of photosystem II light harvesting complexes in eukaryotes. *Biochim. Biophys. Acta* **1817,** 143–157
15. Jansson, S. (1999) A guide to the Lhc genes and their relatives in *Arabidopsis*. *Trends Plant Sci.* **4,** 236–240
16. Caffarri, S., Croce, R., Cattivelli, L., and Bassi, R. (2004) A look within LHCII: differential analysis of the Lhcbl-3 complexes building the major trimeric antenna complex of higher-plant photosynthesis. *Biochemistry* **43,** 9467–9476
17. Dainese, P., and Bassi, R. (1991) Subunit stoichiometry of the chloroplast photosystem-II antenna system and aggregation state of the component chlorophyll-a/b binding proteins. *J. Biol. Chem.* **266,** 8136–8142
18. Boekema, E. J., Van Roon, H., Van Breemen, J. F., and Dekker, J. P. (1999) Supramolecular organization of photosystem II and its light-harvesting antenna in partially solubilized photosystem II membranes. *Eur. J. Biochem.* **266,** 444–452
19. Yakushevska, A. E., Jensen, P. E., Keegstra, W., van Roon, H., Scheller, H. V., Boekema, E. J., and Dekker, J. P. (2001) Supermolecular organization of photosystem II and its associated light-harvesting antenna in *Arabidopsis thaliana*. *Eur. J. Biochem.* **268,** 6020–6028
20. Pagliano, C., Nield, J., Marsano, F., Pape, T., Barera, S., Saracco, G., and Barber, J. (2014) Proteomic characterization and three-dimensional electron microscopy study of PSII-LHCII supercomplexes from higher plants. *Biochim. Biophys. Acta* **1837,** 1454–1462
21. Tokutsu, R., Kato, N., Bui, K. H., Ishikawa, T., and Minagawa, J. (2012) Revisiting the supramolecular organization of photosystem II in *Chlamydomonas reinhardtii*. *J. Biol. Chem.* **287,** 31574–31581
22. Drop, B., Webber-Birungi, M., Yadav, S. K., Filipowicz-Szymanska, A., Fusetti, F., Boekema, E. J., and Croce, R. (2014) Light-harvesting complex II (LHCII) and its supramolecular organization in *Chlamydomonas reinhardtii*. *Biochim. Biophys. Acta* **1837,** 63–72
23. Büchel, C., and Kühlbrandt, W. (2005) Structural differences in the inner part of photosystem II between higher plants and cyanobacteria. *Photosynth. Res.* **85,** 3–13
24. Nield, J., Balsera, M., De Las Rivas, J., and Barber, J. (2002) Three-dimensional electron cryo-microscopy study of the extrinsic domains of the oxygen-evolving complex of spinach: assignment of the PsbO protein. *J. Biol. Chem.* **277,** 15006–15012
25. Wei, X., Su, X., Cao, P., Liu, X., Chang, W., Li, M., Zhang, X., and Liu, Z. (2016) Structure of spinach photosystem II-LHCII supercomplex at 3.2 A resolution. *Nature* **534,** 69–74

Downloaded from http://www.jbc.org/ by guest on June 19, 2019

26. Caffarri, S., Broess, K., Croce, R., and van Amerongen, H. (2011) Excitation energy transfer and trapping in higher plant photosystem II complexes with different antenna sizes. *Biophys. J.* **100,** 2094–2103
27. Galka, P., Santabarbara, S., Khuong, T. T., Degand, H., Morsomme, P., Jennings, R. C., Boekema, E. J., and Caffarri, S. (2012) Functional analyses of the plant photosystem I-light-harvesting complex II supercomplex reveal that light-harvesting complex II loosely bound to photosystem II is a very efficient antenna for photosystem I in state II. *Plant Cell* **24,** 2963–2978
28. Barera, S., Pagliano, C., Pape, T., Saracco, G., and Barber, J. (2012) Characterization of PSII-LHCII supercomplexes isolated from pea thylakoid membrane by one-step treatment with α- and β-dodecyl-D-maltoside. *Philos. Trans. R. Soc. Lond. B Biol. Sci.* **367,** 3389–3399
29. Peter, G. F., and Thornber, J. P. (1991) Biochemical composition and organization of higher plant photosystem II light-harvesting pigment-proteins. *J. Biol. Chem.* **266,** 16745–16754
30. Broess, K., Trinkunas, G., van Hoek, A., Croce, R., and van Amerongen, H. (2008) Determination of the excitation migration time in Photosystem II–consequences for the membrane organization and charge separation parameters. *Biochim. Biophys. Acta* **1777,** 404–409
31. Kouřil, R., Wientjes, E., Bultema, J. B., Croce, R., and Boekema, E. J. (2013) High-light vs. low-light: effect of light acclimation on photosystem II composition and organization in *Arabidopsis thaliana*. *Biochim. Biophys. Acta* **1827,** 411–419
32. Horton, P., Ruban, A. V., Rees, D., Pascal, A. A., Noctor, G., and Young, A. J. (1991) Control of the light-harvesting function of chloroplast membranes by aggregation of the LHCII chlorophyll-protein complex. *FEBS Lett.* **292,** 1–4
33. Schmidt-Krey, I. (2007) Electron crystallography of membrane proteins; two-dimensional crystallization and screening by electron microscopy. *Methods* **41,** 417–426
34. Nogales, E. (2016) The development of cryo-EM into a mainstream structural biology technique. *Nat. Methods* **13,** 24–27
35. Chae, P. S., Rasmussen, S. G., Rana, R. R., Gotfryd, K., Chandra, R., Goren, M. A., Kruse, A. C., Nurva, S., Loland, C. J., Pierre, Y., Drew, D., Popot, J. L., Picot, D., Fox, B. G., Guan, L., *et al.* (2010) Maltose-neopentyl glycol (MNG) amphiphiles for solubilization, stabilization and crystallization of membrane proteins. *Nat. Methods* **7,** 1003–1008
36. Standfuss, J., Terwisscha van Scheltinga, A. C., Lamborghini, M., and Kühlbrandt, W. (2005) Mechanisms of photoprotection and nonphotochemical quenching in pea light-harvesting complex at 2.5A resolution. *EMBO J.* **24,** 919–928
37. Allahverdiyeva, Y., Suorsa, M., Rossi, F., Pavesi, A., Kater, M. M., Antonacci, A., Tadini, L., Pribil, M., Schneider, A., Wanner, G., Leister, D., Aro, E. M., Barbato, R., and Pesaresi, P. (2013) *Arabidopsis* plants lacking PsbQ and PsbR subunits of the oxygen-evolving complex show altered PSII super-complex organization and short-term adaptive mechanisms. *Plant J.* **75,** 671–684
38. Roose, J. L., Frankel, L. K., Mummadisetti, M. P., and Bricker, T. M. (2016) The extrinsic proteins of photosystem II: update. *Planta* **243,** 889–908
39. Shen, J. R., Satoh, K., and Katoh, S. (1988) Isolation of an oxygen-evolving photosystem-Ii preparation containing only one tightly bound calcium atom from a chlorophyll-B-deficient mutant of rice. *Biochim. Biophys. Acta* **936,** 386–394
40. Homann, P. H. (1988) The chloride and calcium requirement of photosynthetic water oxidation–effects of pH. *Biochim. Biophys. Acta* **934,** 1–13
41. Berthold, D. A., Babcock, G. T., and Yocum, C. F. (1981) A highly resolved, oxygen-evolving photosystem II preparation from spinach thylakoid membranes. EPR and electron-transport properties. *FEBS Lett.* **134,** 231–234
42. Kuwabara, T., and Murata, N. (1982) Inactivation of photosynthetic oxygen evolution and concomitant release of 3 polypeptides in the photosystem-Ii particles of spinach-chloroplasts. *Plant Cell Physiol.* **23,** 533–539
43. Miller, M. (1985) The release of polypeptides and manganese from oxygen-evolving photosystem-Ii preparations following zinc-treatment. *FEBS Lett.* **189,** 355–360
44. Enami, I., Kamino, K., Shen, J. R., Satoh, K., and Katoh, S. (1989) Isolation and characterization of photosystem-Ii complexes which lack light-harvesting chlorophyll-a/B proteins but retain 3 extrinsic proteins related to oxygen evolution from spinach. *Biochim. Biophys. Acta* **977,** 33–39
45. Papageorgiou, G. C., and Murata, N. (1995) The unusually strong stabilizing effects of glycine betaine on the structure and function of the oxygen-evolving photosystem-Ii complex. *Photosynth. Res.* **44,** 243–252
46. Caffarri, S., Passarini, F., Bassi, R., and Croce, R. (2007) A specific binding site for neoxanthin in the monomeric antenna proteins CP26 and CP29 of photosystem II. *FEBS Lett.* **581,** 4704–4710
47. Ruban, A. V., Lee, P. J., Wentworth, M., Young, A. J., and Horton, P. (1999) Determination of the stoichiometry and strength of binding of xanthophylls to the photosystem II light harvesting complexes. *J. Biol. Chem.* **274,** 10458–10465
48. Caffarri, S., Croce, R., Breton, J., and Bassi, R. (2001) The major antenna complex of photosystem II has a xanthophyll binding site not involved in light harvesting. *J. Biol. Chem.* **276,** 35924–35933
49. Liu, Z., Yan, H., Wang, K., Kuang, T., Zhang, J., Gui, L., An, X., and Chang, W. (2004) Crystal structure of spinach major light-harvesting complex at 2.72 A resolution. *Nature* **428,** 287–292
50. Grisshammer, R. (2006) Understanding recombinant expression of membrane proteins. *Curr. Opin. Biotechnol.* **17,** 337–340
51. Payandeh, J., Scheuer, T., Zheng, N., and Catterall, W. A. (2011) The crystal structure of a voltage-gated sodium channel. *Nature* **475,** 353–358
52. Faham, S., Boulting, G. L., Massey, E. A., Yohannan, S., Yang, D., and Bowie, J. U. (2005) Crystallization of bacteriorhodopsin from bicelle formulations at room temperature. *Protein Sci.* **14,** 836–840
53. Ujwal, R., Cascio, D., Colletier, J. P., Faham, S., Zhang, J., Toro, L., Ping, P., and Abramson, J. (2008) The crystal structure of mouse VDAC1 at 2.3 A resolution reveals mechanistic insights into metabolite gating. *Proc. Natl. Acad. Sci. U.S.A.* **105,** 17742–17747
54. Vinothkumar, K. R. (2011) Structure of rhomboid protease in a lipid environment. *J. Mol. Biol.* **407,** 232–247
55. Engelmann, E. C., Zucchelli, G., Garlaschi, F. M., Casazza, A. P., and Jennings, R. C. (2005) The effect of outer antenna complexes on the photochemical trapping rate in barley thylakoid photosystem II. *Biochim. Biophys. Acta* **1706,** 276–286
56. Tumino, G., Casazza, A. P., Engelmann, E., Garlaschi, F. M., Zucchelli, G., and Jennings, R. C. (2008) Fluorescence lifetime spectrum of the plant photosystem II core complex: photochemistry does not induce specific reaction center quenching. *Biochemistry* **47,** 10449–10457
57. Croce, R., Canino, G., Ros, F., and Bassi, R. (2002) Chromophore organization in the higher-plant photosystem II antenna protein CP26. *Biochemistry* **41,** 7334–7343
58. Campoli, C., Caffarri, S., Svensson, J. T., Bassi, R., Stanca, A. M., Cattivelli, L., and Crosatti, C. (2009) Parallel pigment and transcriptomic analysis of four barley albina and xantha mutants reveals the complex network of the chloroplast-dependent metabolism. *Plant Mol. Biol.* **71,** 173–191
59. Laemmli, U. K. (1970) Cleavage of structural proteins during the assembly of the head of bacteriophage T4. *Nature* **227,** 680–685
60. Schägger, H. (2006) Tricine-SDS-PAGE. *Nat. Protoc.* **1,** 16–22
61. Tibiletti, T., Auroy, P., Peltier, G., and Caffarri, S. (2016) *Chlamydomonas reinhardtii* PsbS protein is functional and accumulates rapidly and transiently under high light. *Plant Physiol.* 10.1104/pp.16.00572

Downloaded from http://www.jbc.org/ by guest on June 19, 2019

Biochemical and Spectroscopic Characterization of Highly Stable Photosystem II Supercomplexes from *Arabidopsis*

Aurelie Crepin, Stefano Santabarbara and Stefano Caffarri

J. Biol. Chem. 2016, 291:19157-19171.
doi: 10.1074/jbc.M116.738054 originally published online July 18, 2016

Access the most updated version of this article at doi: 10.1074/jbc.M116.738054

Alerts:
- When this article is cited
- When a correction for this article is posted

Click here to choose from all of JBC's e-mail alerts

Supplemental material:
http://www.jbc.org/content/suppl/2016/07/18/M116.738054.DC1

This article cites 61 references, 11 of which can be accessed free at
http://www.jbc.org/content/291/36/19157.full.html#ref-list-1

Downloaded from http://www.jbc.org/ by guest on June 19, 2019